

## Enhancing the photocatalytic activity of commercial P25 TiO<sub>2</sub> powder by combining with handmade Ni-doped TiO<sub>2</sub> powder

Yoshiki Kurokawa, Dang Trang Nguyen, Kozo Taguchi

Department of Science and Engineering, Ritsumeikan University, Japan

---

### Article Info

#### Article history:

Received Apr 15, 2019

Revised Oct 24, 2019

Accepted Nov 4, 2019

---

#### Keywords:

Multilayer thin film

Ni-doped TiO<sub>2</sub> powder

P25 commercial powder

Photocatalyst

Sol-gel method

---

### ABSTRACT

Titanium dioxide (TiO<sub>2</sub>) is the most popular photocatalytic material. However, its operation is limited to UV light only. In this paper, we tried to improve the visible light responsiveness of TiO<sub>2</sub> by doping Nickel (Ni) using the sol-gel method. By combining Ni-doped TiO<sub>2</sub> powder with commercially available P25 TiO<sub>2</sub> powder to make photocatalytic thin films, significant improvement in photocatalytic activity has been obtained. Furthermore, we also studied the relationship between the surface condition of photocatalytic thin films and their photocatalytic activity. The surface condition was improved by the multilayer electrophoresis deposition method. Based on experimental results, by combining 10 20 wt% Ni-doped TiO<sub>2</sub> with P25 TiO<sub>2</sub>, we could significantly enhance the photocatalytic activity of P25 TiO<sub>2</sub>.

Copyright © 2020 Institute of Advanced Engineering and Science.  
All rights reserved.

---

### Corresponding Author:

Kozo Taguchi,

Department of Science and Engineering,

Ritsumeikan University,

1-1-1 Noji-higashi, Kusatsu, Shiga, Japan.

Email: taguchi@se.ritsume.ac.jp

---

## 1. INTRODUCTION

Water quality pollution is becoming an environmental problem all over the world. The causes are domestic and industrial wastewater. Domestic wastewater is wastewater discharged from toilets, baths, and kitchen. Industrial wastewater is drainage from machine processing, food processing factories, etc. Researchers are motivated to solve wastewater problems [1-4]. A photocatalyst is a material that causes a chemical reaction using light energy. It has been used in the energy field, medical field, and environmental field [5, 6]. As photocatalyst materials, titanium dioxide (TiO<sub>2</sub>), cadmium sulfide (CdS), iron (III) oxide (Fe<sub>2</sub>O<sub>3</sub>), tungsten trioxide (WO<sub>3</sub>), zinc oxide (ZnO) are used. Among them, TiO<sub>2</sub> is popularly used due to (1) physically and chemically stable, (2) high photocatalytic activity, (3) non-toxicity, and (4) low price [2, 7, 8]. The sunlight is an important element in the photocatalytic reaction [2, 9]. The light reaching the ground from the sun contains wavelengths in the range from 290 nm to 4000 nm. The range from 100 nm to 400 nm wavelength is called ultraviolet light (UV light), from 400 nm to 800 nm wavelength is called visible light [10]. TiO<sub>2</sub> used as a photocatalyst has 3.2 eV bandgap, so the light having a wavelength shorter than 380 nm (UV light) is required for activating the photocatalytic activity of TiO<sub>2</sub> [11]. The sunlight contains only about 3 - 4 % UV light. Therefore, to increase the photocatalytic efficiency of TiO<sub>2</sub>, research for effective use of the sunlight is necessary [1, 12, 13].

In this research, we tried to improve the photocatalytic activity of TiO<sub>2</sub> by doping nickel to its crystal structure. To make Ni-doped TiO<sub>2</sub>, we used the sol-gel method [14]. Thin films of TiO<sub>2</sub> were fabricated by the electrophoresis deposition (EPD) method. Thin films made of commercially available P25 TiO<sub>2</sub> powder combined with the handmade Ni-doped TiO<sub>2</sub> powder were investigated to improve the photocatalytic efficiency. Methylene blue (MB) degradation experiment was used to characterize the photocatalytic efficiency of the fabricated thin films.

## 2. RESEARCH METHOD

### 2.1. Fabricating Ni-doped TiO<sub>2</sub> powder by sol-gel method

The sol-gel process is a method for producing solid particles from molecules. Hydrolysis and polycondensation reactions are repeated in sol solution and gel state. Then, the gel is dried and undergone heat treatment. The advantage of this method is that it can be applied to organic and inorganic molecule hybrid materials. The preparation of TiO<sub>2</sub> powder by this method can be represented by the following equation [15, 16].



To synthesize Ni-doped TiO<sub>2</sub> powder by sol-gel method, we mixed 6 ml titanium tetraisopropoxide (Wako, Japan), 20 ml ethanol (Wako, Japan), 1 ml deionized water (Wako, Japan), and 0.029 g Ni(NO<sub>3</sub>)<sub>2</sub> · 6H<sub>2</sub>O (Wako, Japan) in a glass beaker using a magnetic stirrer (ASONE, RS-6DN) rotating at the speed of 500 rpm for 1 hour. Then, the prepared solution was dried at 100 °C for about 3 hours. After that, the obtained dried gel was ground in a mortar to become a fine powder. The powder was annealed at 650 °C for 1 hour with an electric furnace (ASONE SMF-1) to obtain crystalline Ni-doped TiO<sub>2</sub> powder (light yellow color) [13, 17-19]. This powder is called as Ni-SP powder.

### 2.2. Fabricating TiO<sub>2</sub> thin film by EPD method

EPD method is a method used for depositing minute particles on a conducting substrate by an external electric field. Based on this method, a thin film with controllable thickness can be produced. Under an applied external electric field, TiO<sub>2</sub> particles in a colloid solution are positively charged and moved to the negatively charged electrode [20-23]. Commercially available P25 TiO<sub>2</sub> powder (particle size: 20 nm) and a suitable amount of fabricated Ni-SP powder were mixed with ethanol at the speed of 700 rpm for 1 hour by a magnetic stirrer to make a colloid solution for EPD. Figure 1 shows the setup used for conducting EPD. An aluminum plate (used as the anode electrode (20 × 20 × 1 mm)) and an FTO glass (used as the cathode electrode (20 × 20 × 1.8 mm)) were placed at 10 mm in parallel into the prepared colloid solutions. To conduct EPD, a constant current of 0.12 mA (generated by a current source, ADVANTEST R6144) was applied to the two electrodes.

To make single-layer thin films, EPD was conducted 100 seconds continuously. On the other hand, to make multilayer thin films (four layers), EPD was conducted four times; each time lasted 25 seconds followed by drying at 60°C for 1 minute. The deposited areas on FTO substrates were 10×20 mm. After completing deposition, as-fabricated thin films were annealed in the air at 400°C (5°C/minute heating rate) for 1 hour. Both single-layer and four-layer thin films had the same thickness of about 15 μm. Moreover, a scanning electron microscope (SEM, HITACHI S4300) was used to observe Ni-SP powder, single-layer thin film surface, and multilayer thin film surface. An X-ray diffraction spectroscopy (XRD, PANalytical) was used to measure crystalline morphology and quantitative analysis of P25 powder and Ni-SP powder. A UV-vis spectrophotometer (SHIMAZU, UV-3600) was used to evaluate the light absorption band of the fabricated thin films.

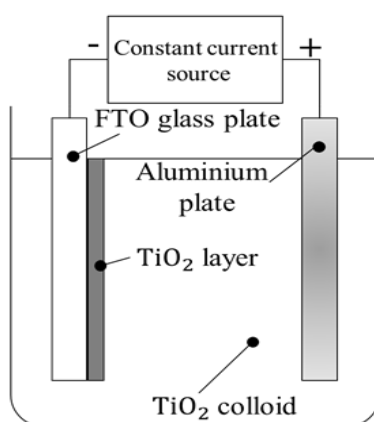


Figure 1. Setup for conducting EPD

### 2.3. Photocatalytic activity and photocatalytic degradation of MB

The operation principle of  $\text{TiO}_2$  working as a photocatalyst is shown in Figure 2. Assuming that  $\text{TiO}_2$  is put in a solution containing organic matters. When UV light irradiates to photocatalytic  $\text{TiO}_2$ , electrons are excited from the valence band to the conduction band. Positive holes are present in the valence band ( $h_{\text{VB}}^+$ ) and electrons are present in the conduction band ( $e_{\text{CB}}^-$ ) as shown in (2). Positive holes deprive electrons of the (OH) group of water in contact with the photocatalyst surfaces. Hydroxide ions are deprived of electrons and become hydroxyl radicals. Hydroxyl radicals take electrons from nearby organic matter to change from an unstable state to a stable state as shown in (3). Electrons in the conduction band reduce oxygen to superoxide anions ( $\text{O}_2^{\cdot -}$ ) as shown in (4). Hydroxyl radical and superoxide anion are called reactive oxygen and they have strong oxidizing power. They attack organic matter presence near the surfaces of the photocatalyst. Ultimately, this process causes complete degradation of organic matters into harmless molecules [3, 24].

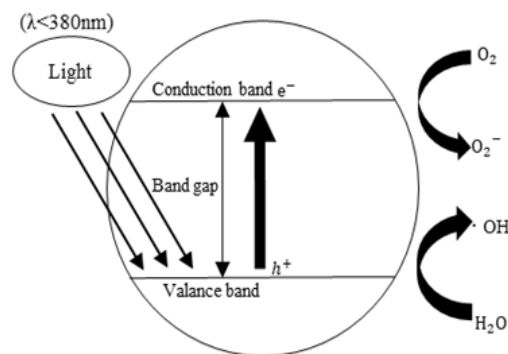
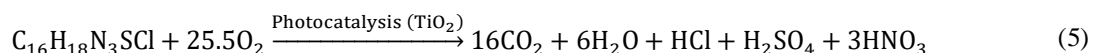


Figure 2. Photocatalytic operation principle of  $\text{TiO}_2$

The photocatalytic activity of the fabricated thin films was evaluated based on their MB degradation rates. MB photocatalytic decomposition can be represented as shown in (5). This experiment was performed using  $10 \mu\text{M}$  MB dye solution illuminated by a UV light source (TOSHIBA, FL20S-BL lamp), which illuminates UV light and little visible light (400 - 500 nm). As shown in Figure 3, small transparent plastic containers were filled with 5 ml of the MB solution. Then, the fabricated thin films were immersed in these containers. After that, they were irradiated by the UV lamp with a 5 cm distance from the lamp. Every one-hour interval, 1 ml solution was taken out of each container for measuring the transmittance by a UV-vis spectrophotometer. After the measurement, we returned the taken-out solution to the corresponding container for further photocatalytic degradation experiments. We repeated the measurement six times in total. The absorbance (ABS) can be expressed as shown in (6) using the measured transmittance. The MB degradation rate is proportional to the absorbance, which is calculated using a shown in (7) [1, 2, 25].



$$\text{Absorbance (ABS)} = \ln(T_0/T_t) \quad (6)$$

where,  $T_0$ : initial transmittance and  $T_t$ : Transmittance at a given time

$$\text{MB degradation rate (\%)} = (\text{ABS}_0 - \text{ABS}_t)/\text{ABS}_0 \times 100 \quad (7)$$

where,  $\text{ABS}_0$  and  $\text{ABS}_t$  are the concentrations of the MB solution at time 0 and t, respectively

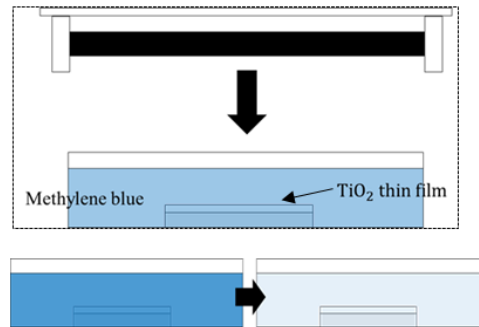


Figure 3. Top diagram: experimental setup of the MB degradation experiment.  
Bottom diagram: before light exposure (left) and after light exposure (right)

### 3. RESULTS AND ANALYSIS

#### 3.1. Powder characterization

SEM images at different magnification of Ni-SP powder shown in Figure 4. SEM images of Ni-SP powder are shown in Figure 4. The diameter of Ni-SP particles is estimated about 100 nm. Therefore, Ni-SP particles are about 5 times larger than P25 particles (20 nm diameter). Figure 5 shows the XRD measurement data of Ni-SP and P25 powders. These powders have strong diffraction peaks in anatase and rutile crystal forms. Anatase peaks recognized at  $25.27^\circ$ ,  $37.76^\circ$ ,  $38.56^\circ$ ,  $48.05^\circ$ ,  $53.88^\circ$ ,  $55.00^\circ$ ,  $62.19^\circ$ ,  $68.73^\circ$ ,  $70.34^\circ$ ,  $75.12^\circ$  [26]. Generally,  $\text{TiO}_2$  anatase causes photocatalytic reactions. Furthermore, Ni-SP powder showed two peaks at  $33.13^\circ$  and  $49.48^\circ$  that were absence in P25 powder. These are two peaks of  $\text{NiTiO}_3$  [27]. Based on the result of the quantitative analysis of XRD data, Ni-SP contained 74 % of anatase, 12 % of rutile, and 14 % of  $\text{NiTiO}_3$  while P25 contained 79 % of anatase and 21 % of rutile. From these results, it can be inferred that the nickel-doped  $\text{TiO}_2$  was successfully synthesized by the sol-gel method.

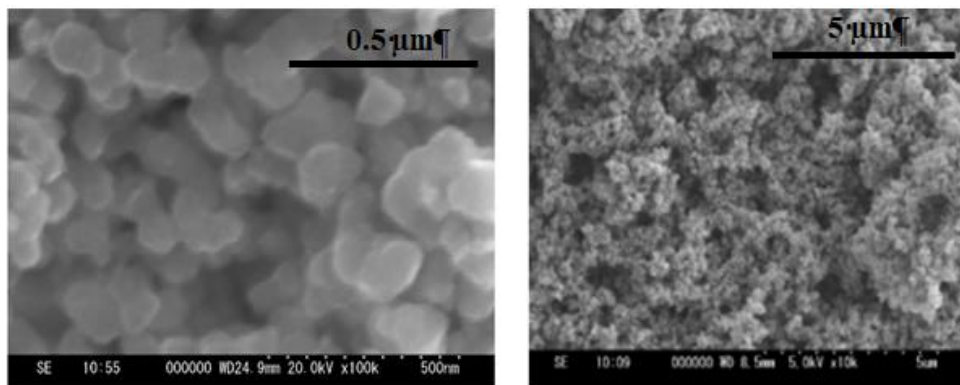


Figure 4. SEM images at a different magnification of Ni-SP powder

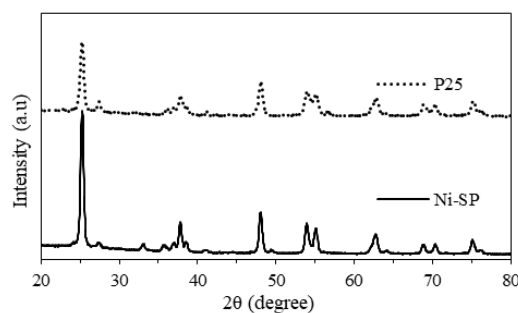


Figure 5. XRD diffraction patterns of Ni-SP and P25 powders

### 3.2. Single-layer thin films

#### 3.2.1 Single-layer thin films of P25 and Ni-SP

UV-vis spectra of the single-layer thin films of P25 and Ni-SP are shown in Figure 6. The P25 thin-film absorbed only light with wavelength shorter than 400 nm (UV light). This light-absorbing characteristic is originally possessed by TiO<sub>2</sub>. On the other hand, the Ni-SP thin-film absorbed light with wavelength shorter than 400 nm and wavelength from 400 to 500 nm. From this result, it can be confirmed that doping Ni to TiO<sub>2</sub> can extend the absorption band of TiO<sub>2</sub> to little visible light.

The MB degradation rates of the single-layer thin films of P25 and Ni-SP are displayed in Figure 7. A surprising result has been obtained. Although the Ni-SP thin film could absorb a larger light band than the P25 thin film, the higher degradation rate was obtained with the P25 thin film with 62.31 % after 6-hour light exposure while the Ni-SP thin film showed the lower degradation rate of 47.83 % after 6-hour light exposure. This result may be attributed to larger particle size of Ni-SP (5 times) leading to lower surface area; and lower anatase crystal ratio than P25 (anatase is the main cause of photocatalytic reaction).

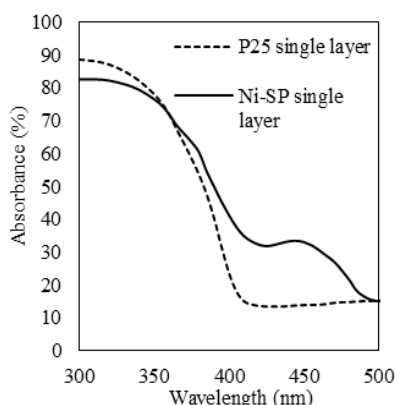


Figure 6. UV-vis spectra of single-layer thin films of P25 and Ni-SP

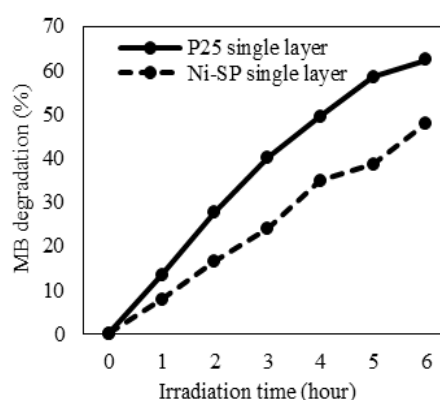


Figure 7. Photocatalytic degradation rates of MB dye by single-layer thin films of P25 and Ni-SP

#### 3.2.2. Combining Ni-SP with P25 to improve the overall photocatalytic activity

To utilize the larger light absorption band of Ni-SP, we tried to enhance the overall photocatalytic activity by combining Ni-SP with P25. Table 1 shows single-layer thin-film samples made of different ratios of Ni-SP and P25 powders. The SEM images of the surfaces of samples A, C, E, and G are shown in Figure 8 (A), (C), (E), and (G), respectively. Because of the single-layer structure, many cracks could be observed on these samples' surfaces [28].

UV-vis spectra of samples A (Ni-SP only), E (combining Ni-SP and P25), and G (P25 only) are shown in Figure 9. Obviously, sample E showed the combining characteristics of samples A and G with high light absorbance in UV light and little absorbance in visible light (400 – 500 nm). Figure 10 shows the MB degradation rates as a function of light exposure time obtained with samples A - G. In the same light exposure period, sample E (P25 83 wt% and Ni-SP 17 wt%) showed the highest MB degradation rate of 68.84 %. Meanwhile, sample A (Ni-SP only) showed the lowest MB degradation rate of 47.83 %. In addition, samples B, C, D, F, G showed the MB degradation rates of 51.61 %, 56.03 %, 62.80 %, 67.55 %, 62.31 %, respectively. Comparing sample E and sample G, the MB degradation rate has been improved about 10.0 %. Based on this experiment, it can be confirmed that by mixing about 10 - 20 wt% Ni-SP to P25, we could enhance the overall photocatalytic activity of the commercial P25 powder.

Table 1. Single-layer samples made of different ratios of Ni-SP and P25 powders

Sample	P25 (wt%)	Ni-SP (wt%)	Layer
A	0	100	Single layer
B	16	84	Single layer
C	50	50	Single layer
D	66	34	Single layer
E	83	17	Single layer
F	91	9	Single layer
G	100	0	Single layer

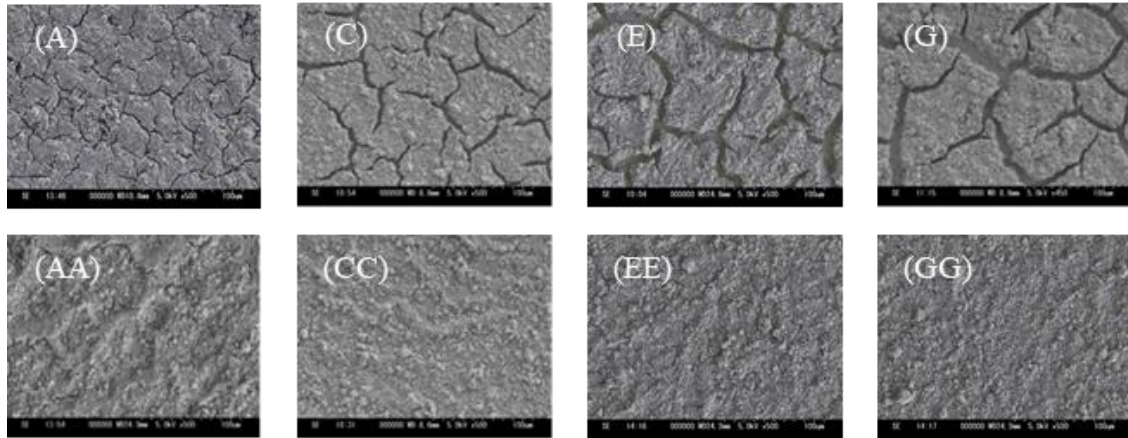


Figure 8. SEM images of some single-layer thin films ((A), (C), (E), and (G) represent samples A, C, E, and G, respectively) and four-layer thin films ((AA), (CC), (EE), and (GG) represent samples AA, CC, EE, and GG, respectively)

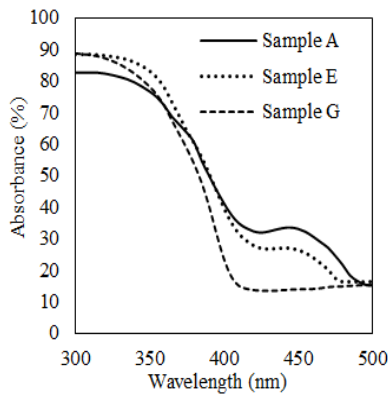


Figure 9. UV-vis spectra of samples A, E, and G

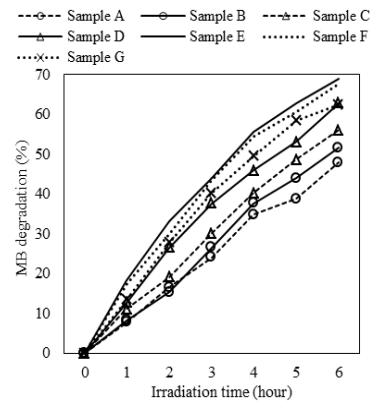


Figure 10. Photocatalytic degradation rates of MB dye by samples A – G

**3.3. Multilayer thin films (four layers)**

In order to reduce cracks on the thin-film surface, we fabricated multilayer thin films with a four-layer structure. Table 2 shows multilayer thin-film samples made of different ratios of Ni-SP and P25 powders (the same ratios as samples in Table 1. The MB degradation experiment was also conducted using these multilayer thin films. Figure 8 shows SEM images of the surfaces of samples A, C, E, G, AA, CC, EE, GG. The single-layer thin films had many cracks on their surface Figure 8 (A), (C), (E), and (G). These cracks caused to reduce the surface area of these thin films. On the other hand, there was almost no crack observed on the surfaces of the four-layer thin films Figure 8 (AA) (CC) (EE) (GG). It can be confirmed that the multilayer fabrication method can improve the quality of the thin films.

Table 2. Multilayer samples made of different ratios of Ni-SP and P25 powders

Sample	P25 (wt%)	Ni-SP (wt%)	Layer
AA	0	100	Four layers
BB	16	84	Four layers
CC	50	50	Four layers
DD	66	34	Four layers
EE	83	17	Four layers
FF	91	9	Four layers
GG	100	0	Four layers

The MB degradation rates of samples AA – GG are shown in Figure 11. Similar to the single-layer thin films, sample EE (P25 83 wt% and Ni-SP 17 wt%) also had the highest MB degradation rate of 75.83 %. Meanwhile, sample AA (Ni-SP only) also had the lowest MB degradation rate of 54.47%. The MB degradation rates of samples BB, CC, DD, FF, GG were 54.96 %, 61.13 %, 65.61 %, 75.23 %, 67.30 %, respectively. By combining Ni-SP with P25, the MB degradation rate could be improved 12.6 % (comparing sample EE with sample GG). All samples with four layers achieved higher MB degradation rates than that of the single-layer samples. If comparing sample E and sample EE, the MB degradation rate has been improved by about 10.0 % (from 68.84 % to 75.83 %).

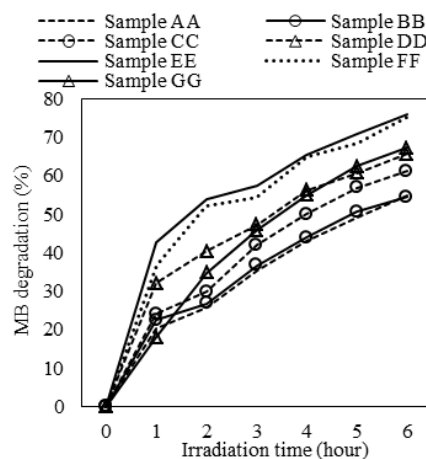


Figure 11. Photocatalytic degradation rates of MB dye by samples AA-GG

#### 4. CONCLUSION

In this paper, we used Ni-doped TiO<sub>2</sub> powder fabricated by the sol-gel method to enhance the photocatalytic activity of commercial P25 TiO<sub>2</sub> powder. Multilayer EPD fabrication method was also utilized to improve the quality of the thin films, as a result, the higher MB degradation rates have been obtained. The handmade Ni-SP powder showed visible light absorbance (400-500 nm). Because of large particle size (~ 100 nm), Ni-SP thin films achieved low photocatalytic activity if compared with P25 thin films. However, by combining a suitable amount of Ni-SP with P25, significant improvement in photocatalytic activity could be obtained.

#### REFERENCES

- [1] M. B. Fisher, D. A. Keane, P. Fernández-Ibáñez, J. Colreavy, S. J. Hinder, K. G. McGuigan, and S. C. Pillai, "Nitrogen and copper doped solar light active TiO<sub>2</sub> photocatalysts for water decontamination," *Appl. Catal. B Environ.*, vol. 130, pp. 8–13, 2013.
- [2] Ö. Kerkez-Kuyumcu, E. Kibar, K. Dayioğlu, F. Gedik, A. N. Akın, and Ş. Özkara-Aydınoğlu, "A comparative study for removal of different dyes over M/TiO<sub>2</sub> (M=Cu, Ni, Co, Fe, Mn and Cr) photocatalysts under visible light irradiation," *J. Photochem. Photobiol. A Chem.*, vol. 311, pp. 176–185, 2015.
- [3] M. Y. Ghaly, T. S. Jamil, I. E. El-Seesy, E. R. Souaya, and R. A. Nasr, "Treatment of highly polluted paper mill wastewater by solar photocatalytic oxidation with synthesized nano TiO<sub>2</sub>," *Chem. Eng. J.*, vol. 168, no. 1, pp. 446–454, Mar. 2011.
- [4] P. A. Pekakis, N. P. Xekoukoulotakis, and D. Mantzavinos, "Treatment of textile dyehouse wastewater by TiO<sub>2</sub> photocatalysis," *Water Res.*, vol. 40, no. 6, pp. 1276–1286, Mar. 2006.
- [5] H. Hu, W. Xiao, J. Yuan, J. Shi, M. Chen, and W. Shang Guan, "Preparations of TiO<sub>2</sub> film coated on foam nickel substrate by sol-gel processes and its photocatalytic activity for degradation of acetaldehyde," *J. Environ. Sci.*, vol. 19, no. 1, pp. 80–85, Jan. 2007.
- [6] G. Kenanakis, D. Vernardou, A. Dalamagkas, and N. Katsarakis, "Photocatalytic and electrooxidation properties of TiO<sub>2</sub> thin films deposited by sol-gel," *Catal. Today*, vol. 240, pp. 146–152, Feb. 2015.
- [7] W.-C. Hung, S.-H. Fu, J.-J. Tseng, H. Chu, and T.-H. Ko, "Study on photocatalytic degradation of gaseous dichloromethane using pure and iron ion-doped TiO<sub>2</sub> prepared by the sol-gel method," *Chemosphere*, vol. 66, no. 11, pp. 2142–2151, Feb. 2007.

- [8] L. Jing, B. Xin, F. Yuan, L. Xue, A. Baiqi Wang, and H. Fu, "Effects of surface oxygen vacancies on photophysical and photochemical processes of Zn-doped TiO<sub>2</sub> nanoparticles and their relationships," *J. Phys. Chem. B*, vol. 110, no. 36, pp. 17860–17865, 2006.
- [9] R. S. Dariani, A. Esmaili, A. Mortezaali, and S. Dehghanpour, "Photocatalytic reaction and degradation of methylene blue on TiO<sub>2</sub> nano-sized particles," *Optik (Stuttg.)*, vol. 127, no. 18, pp. 7143–7154, 2016.
- [10] M. P. Blanco-Vega, J. L. Guzmán-Mar, M. Villanueva-Rodríguez, L. Maya-Treviño, L. L. Garza-Tovar, A. Hernández-Ramírez, L. Hinojosa-Reyes, "Photocatalytic elimination of bisphenol A under visible light using Ni-doped TiO<sub>2</sub> synthesized by microwave assisted sol-gel method," *Mater. Sci. Semicond. Process.*, vol. 71, no. May, pp. 275–282, 2017.
- [11] M. Mashkour, M. Rahimnejad, S. M. Pourali, H. Ezoji, A. ElMekawy, and D. Pant, "Catalytic performance of nano-hybrid graphene and titanium dioxide modified cathodes fabricated with facile and green technique in microbial fuel cell," *Prog. Nat. Sci. Mater. Int.*, vol. 27, no. 6, pp. 647–651, Dec. 2017.
- [12] R. S. Sonawane, B. B. Kale, and M. K. Dongare, "Preparation and photo-catalytic activity of Fe-TiO<sub>2</sub> thin films prepared by sol-gel dip coating," *Mater. Chem. Phys.*, vol. 85, no. 1, pp. 52–57, 2004.
- [13] T. C. Jagdale, S. P. Takale, R. S. Sonawane, H. M. Joshi, S. I. Patil, B. B. Kale, and S. B. Ogale, "N-Doped TiO<sub>2</sub> nanoparticle based visible light photocatalyst by modified peroxide sol-gel method," *J. Phys. Chem. C*, vol. 112, no. 3, pp. 14595–14602, 2008.
- [14] Y. Kurokawa, D. T. Nguyen, and K. Taguchi, "Nickel-doped TiO<sub>2</sub> multilayer thin film for enhancement of photocatalytic activity," *Int. J. Mater. Sci. Eng.*, vol. 7, no. 1, pp. 10–19, 2019.
- [15] K. Pomoni, A. Vomvas, and C. Trapalis, "Electrical conductivity and photoconductivity studies of TiO<sub>2</sub> sol-gel thin films and the effect of N-doping," *J. Non. Cryst. Solids*, vol. 354, no. 35, pp. 4448–4457, 2008.
- [16] U. G. Akpan and B. H. Hameed, "The advancements in sol-gel method of doped-TiO<sub>2</sub> photocatalysts," *Appl. Catal. A Gen.*, vol. 375, no. 1, pp. 1–11, 2010.
- [17] G. Liu, X. Zhang, Y. Xu, X. Niu, L. Zheng, and X. Ding, "The preparation of Zn<sup>2+</sup>-doped TiO<sub>2</sub> nanoparticles by sol-gel and solid phase reaction methods respectively and their photocatalytic activities," *Chemosphere*, vol. 59, no. 9, pp. 1367–1371, 2005.
- [18] H. Yu, X. J. Li, S. J. Zheng, and W. Xu, "Photocatalytic activity of TiO<sub>2</sub> thin film non-uniformly doped by Ni," *Mater. Chem. Phys.*, vol. 97, no. 1, pp. 59–63, 2006.
- [19] G. G. Nakhate, V. S. Nikam, K. G. Kanade, S. Arbuji, B. B. Kale, and J. O. Baeg, "Hydrothermally derived nanosized Ni-doped TiO<sub>2</sub>: A visible light driven photocatalyst for methylene blue degradation," *Mater. Chem. Phys.*, vol. 124, no. 2–3, pp. 976–981, 2010.
- [20] S. Novak, U. Maver, Š. Peternel, P. Venturini, M. Bele, and M. Gaberšček, "Electrophoretic deposition as a tool for separation of protein inclusion bodies from host bacteria in suspension," *Colloids Surfaces A Physicochem. Eng. Asp.*, vol. 340, no. 1–3, pp. 155–160, 2009.
- [21] S. Bhardwaj, A. Pal, K. Chatterjee, P. Chowdhury, S. Saha, A. Barman, T. H. Rana, G. D. Sharma, and S. Biswas, "Electrophoretic deposition of plasmonic nanocomposite for the fabrication of dye-sensitized solar cells," *Indian J. Pure Appl. Phys.*, vol. 55, no. 1, pp. 73–80, 2017.
- [22] A. S. Shikoh, Z. Ahmad, F. Touati, R. A. Shakoob, and S. A. Al-Muhtaseb, "Optimization of ITO glass/TiO<sub>2</sub> based DSSC photo-anodes through electrophoretic deposition and sintering techniques," *Ceram. Int.*, vol. 43, no. 13, pp. 10540–10545, 2017.
- [23] C. Rama Krishna, W. M. Lee, S. Y. Oh, K. U. Jeong, and Y. T. Yu, "Improvement in light harvesting and device performance of dye sensitized solar cells using electrophoretic deposited hollow TiO<sub>2</sub> NPs scattering layer," *Sol. Energy Mater. Sol. Cells*, vol. 161, no. December 2016, pp. 255–262, 2017.
- [24] M. A. Ahmed, "Synthesis and structural features of mesoporous NiO/TiO<sub>2</sub> nanocomposites prepared by sol-gel method for photodegradation of methylene blue dye," *J. Photochem. Photobiol. A Chem.*, vol. 238, pp. 63–70, 2012.
- [25] Y. Zhang and Q. Li, "Synthesis and characterization of Fe-doped TiO<sub>2</sub> films by electrophoretic method and its photocatalytic activity toward methyl orange," *Solid State Sci.*, vol. 16, pp. 16–20, 2013.
- [26] H. C. Chang, M. J. Twu, C. Y. Hsu, R. Q. Hsu, and C. G. Kuo, "Improved performance for dye-sensitized solar cells using a compact TiO<sub>2</sub> layer grown by sputtering," *Int. J. Photoenergy*, vol. 23, pp. 1–8, 2014.
- [27] Y. J. Lin, Y. H. Chang, W. D. Yang, and B. S. Tsai, "Synthesis and characterization of ilmenite NiTiO<sub>3</sub> and CoTiO<sub>3</sub> prepared by a modified Pechini method," *J. Non. Cryst. Solids*, vol. 352, no. 8, pp. 789–794, Jun. 2006.
- [28] Y. Kurokawa, D. T. Nguyen, and K. Taguchi, "Optimum conditions for titanium oxide thin film on dye-sensitized solar cells using organic dye sensitizer-MK2," *Int. J. Chem. Eng. Appl.*, vol. 9, no. 6, pp. 200–205, 2018.

## BIOGRAPHIES OF AUTHORS



**Yoshiki Kurokawa** was born in Shiga, Japan on April 26, 1994. He received bachelor's degree in Department of Science and Engineering from Ritsumeikan University, Shiga, Japan in March 2017 and was admitted to a postgraduate course at same University on April 2017. He also belongs to an electronics system course of Department of Science and Engineering. He is now in the second year. He is making a study of photocatalyst by using electrophoresis deposition in the graduate course.





**D. Trang Nguyen** was born in Vietnam in 1986. He received the BS degree in 2009 from the Department of Telecommunication Systems Hanoi University of Science and Technology, Hanoi, Vietnam. After that, he received the ME in 2011 from the Department of Electronics and Electrical Engineering, Dongguk University, Seoul, South Korea. From 2011 to 2014, he completed his Ph. D program in integrated science and engineering at Ritsumeikan University, Kyoto, Japan. After earning his Ph. D, he was a quality assurance engineer at Takako Industries, Inc. from 2015 to 2017. Currently, he is a senior researcher at the Ritsumeikan Global Innovation Research Organization, Ritsumeikan University. His fields of interest include Biofuel Cells, Solar Cells, Biosensors, and Hydrogen Energy.



**Kozo Taguchi** was born in Kyoto, Japan, on December 18, 1968. He received the B.E., M.E., and Dr. Eng. Degrees in electrical engineering from Ritsumeikan University, Kyoto, Japan, in 1991, 1993, and 1996, respectively. In 1996, he joined Fukuyama University, Hiroshima, Japan, where he had been engaged in research and development on the optical fiber trapping system, semiconductor ring lasers and their application for optoelectronics devices, and polymeric optical waveguides for optical interconnection. In 1996–2003, he worked as an assistant and lecturer in Fukuyama University. In 2003, he moved to Ritsumeikan University, Shiga, Japan, and currently he is a professor of department of electric and electronic engineering. From 2006 to 2007, he was a visiting professor at University of St Andrews (Scotland, United Kingdom). From 2014 to 2015, he was a visiting professor at Nanyang Technological University (Singapore). In 2019, he was a visiting professor at University of Bath (United Kingdom). His current research interests include cells trap, microfluidic cell-based devices, dye sensitized solar cell, biofuel cells, biosensors, and hydrogen energy. Dr. Taguchi is a member of the JJAP.